Atomic beam slowing and cooling: Discrete velocity model

C. Reitshammer and F. Schürrer
Institut für Theoretische Physik, Technische Universität Graz, Petersgasse 16, A-8010 Graz, Austria

A. Rossani
Dipartimento di Matematica, Politecnico di Torino, Corso Duca Abruzzi 24, I-10129 Torino, Italy
(Received 25 November 1997; revised manuscript received 16 April 1998)

A discrete velocity model of the Boltzmann equation is established to investigate the effect of atomic beam slowing and cooling by means of laser light. Due to momentum transfer, caused by absorption and emission processes of photons, atoms are slowed. The Doppler effect, however, allows only selected atoms within a certain resonance range to interact with the laser field. To overcome this problem an external electric field is maintained. Semianalytical results of the velocity distribution as a function of the deceleration path of both ground level atoms and excited atoms are presented in detail and studied explicitly for various values of the laser intensity. A cooling limit is given and compared with quantum mechanical results.
[S1063-651X(98)03609-5]

PACS number(s): 02.70.−c, 05.20.Dd, 32.80.Pj

I. INTRODUCTION

The particle distribution function of dilute gases in equilibrium and nonequilibrium states is described by the Boltzmann equation [1]. In its extended form not only elastic but also inelastic interactions can be dealt with [2]. The interaction of a gas with a radiation field has been studied in the past mainly by means of a continuum approach [3,4]. A useful introduction to the kinetic theory of particles interacting with photons is given by Oxenius [5]. Current research expands upon the original Boltzmann equation in a way that elastic and inelastic terms for particle-particle collisions are introduced and the evolution of the radiation field is taken into account by means of a kinetic equation for photons [6]. These complicated systems of Boltzmann-like differential and integro-differential equations are very difficult to solve.

One way out of this problem is the discretization of the velocity space [7,8]. Early discrete velocity models of the continuous Boltzmann equation refer to idealized gases with only one or two particle speeds [9–11]. This was a big shortcoming because the temperature was ill defined and it was exaggerated to speak of a velocity distribution when only two velocity moduli were involved. The physical discrete models, however, are the multispeed ones [12].

In the case of atomic beam slowing and cooling the atoms of the beam interact with counterpropagating laser photons. The atoms are slowed on grounds of momentum transfer caused by absorption and emission processes. Due to the Doppler effect only selected atoms within the resonance range are able to absorb photons. An external electrical field is maintained, holding atoms in resonance by utilizing the Stark effect. Therefore, atomic beam slowing and cooling is a fascinating challenge for applying discrete kinetic models to investigate the space dependence of the velocity distribution of the atoms within the beam.

Several theoretical papers [13,14] treat the problem of atomic beam cooling mainly from a quantum mechanical point of view. Starting with Wigner-Bloch equations, laser cooling can be described by means of a Monte Carlo simulation. In addition, statistical methods have been used to gain insight into the process of resonant atom-photon interactions. Although by applying the Fokker-Planck equation (FPE) [15–17] a realistic discussion of cooling in a Gaussian laser beam seems to be promising, no general solutions of this equation have been reported up to now. For a Gaussian laser beam this FPE is at least a five-variable partial differential equation with two spatial and two velocity coordinates (longitudinal and transverse) and an explicit time dependence. This multivariable dependence combined with an extremely rapid variation of the distribution function with the velocity makes a direct (numerical) integration of this equation very difficult [18]. Wallis and Ertmer [19] analyzed atomic beam deceleration with time-dependent drift and diffusion coefficients and compared different theoretical approaches.

In this paper we analyze atomic beam cooling by applying a discrete velocity model of the Boltzmann equation. Because of the very little momentum transfer of the atom-photon interaction, we use a sufficiently fine equidistant grid in the velocity space to obtain a realistic simulation of the cooling process. We study stationary states of the number densities of both ground state atoms and excited atoms. There are two aspects why we investigate it by means of a discrete velocity model. First, we demonstrate that the discrete Boltzmann equation yields an alternative description to quantum Monte Carlo methods and second, we want to gain insight into the influence of the laser intensity. An essential advantage of our method is, in contrast to the quantum mechanical treatment, that we can predict the velocity distribution of the atomic beam at all points of the deceleration path. Furthermore, we are able to take into account the real atomic and laser profiles and every kind of influence on the energy levels of the atoms of the beam (Stark effect or Zeemann effect) by introducing a space- and velocity-dependent cross-section-like function into our model.

In dealing with laser cooling, our model yields a system of linear first-order differential equations. Normally, Runge-Kutta algorithms apply to solve such a system. However, due to the above-mentioned rapid variation of the distribution

function, it is impossible to obtain physically relevant solutions. We therefore stratify the deceleration path and connect the layers by taking the ''end densities'' as initial data for the next layer. The discretization of the folded atomic Lorentz and the Gaussian laser profile leads to a system of linear differential equations with constant coefficients. The subsequent solution of this system of differential equations for each layer yields the number densities as superpositions of exponential functions. Our formalism not only gives a straightforward intuitive interpretation of resonant radiation pressure, allowing us to visualize the random walk and internal dynamics of an atom in a propagating external light wave, but also shows us how to implement this picture in a numerical simulation of the distribution function.

Section II describes the general model in two dimensions of the velocity space. Section III reduces the problem to one-dimensional solutions. The semianalytical results are discussed in Sec. IV. We conclude in Sec. V.

II. GENERAL MODEL

A. Physical situation

The physical system consists of ground level atoms A, excited atoms A^*, and photons p. The mass of the atoms (A and A^*) is assumed to be almost the same: m. We call E_{12} the energy jump between the two internal energy levels. Photons p are assumed to be at a fixed frequency ν_L. Atoms and photons interact within an infinite slab $x\in[0,L]$. At a position $x=0$ and for $y\in[-h_1,h_1]$ particles A are continuously injected with a direction normal to the slab. These atoms follow a given velocity distribution. At a position $x=L$ and for $y\in[-h_2,h_2]$ (where $h_2>h_1$), photons at a frequency ν_L are continuously injected within a direction normal to the slab and are counterpropagating to the atoms. We consider the following interaction events between atoms and photons: absorption, $A+p\rightarrow A^*$; spontaneous emission, $A^*\rightarrow A+p'$; and stimulated emission, $A^*+p\rightarrow A+2p$. Absorption and stimulated emission are described by means of the same Einstein-Milne absorption coefficient B_{12}. The decay constant of spontaneous emission is given by A_{21}.

In our model the specific intensity $I_\nu(\mathbf{r},\mathbf{\Omega},t)$ of impinging photons is characterized by

$$I_\nu(\mathbf{r},\mathbf{\Omega},t)=I(\mathbf{r},\mathbf{\Omega},t)\,\delta(\nu-\nu_L'), \tag{1}$$

which states the laser profile. The quantity $I(\mathbf{r},\mathbf{\Omega},t)$ is the intensity of the laser beam in direction $\mathbf{\Omega}$. The quantity

$$\nu_L'=\nu_L\left(1+\frac{v_x}{c}\right) \tag{2}$$

denotes the laser frequency with reference to a moving atom due to the Doppler effect, where $v_x=\mathbf{v}\cdot\mathbf{i}$ and c is the speed of light. The atomic profile $\alpha_{12}(\nu)$ (in the rest frame of the atom) is a Lorentz profile given by

$$\alpha_{12}(\nu)=\frac{d_2/\pi}{(\nu-\nu_0)^2+d_2^2}, \tag{3}$$

where d_2 measures the natural linewidth of the profile and ν_0 is the transition frequency.

Hence, due to the Doppler effect, only a few atoms within a velocity interval $v_{res}\pm\Delta v$ are able to interact with photons. However, we want to slow down almost all atoms within the slab and for this reason, for $x\in[0,L]$ an electric field $\mathbf{E}(x)=\mathbf{j}E(x)$ is introduced to compensate for the Doppler effect. Here $\mathbf{i}$ and $\mathbf{j}$ are unit vectors in the x and y directions, respectively. Due to the Stark effect, the internal energy jump E_{12} depends on x through $E(x)$ so that the transition frequency ν_0 becomes a function of x: $\nu_0(x)=E_{12}(x)/h$ (where h is Planck's constant). We assume that $E_{12}(x)$ is a given, monotonically decreasing, function of x, for example,

$$E_{12}(x)=c_1(1-c_2x), \tag{4}$$

with positive constants c_1 and c_2.

The interaction between atoms and photons leads to a folding

$$F=B_{12}\int_{\nu=0}^{\infty}d\nu\int_{\Omega=0}^{4\pi}d\Omega\,\frac{1}{4\pi}I_\nu(\mathbf{r},\mathbf{\Omega},t)\,\alpha_{12}(\nu)$$

$$=b(x,v_x)\int_{\Omega=0}^{4\pi}d\Omega\;I(\mathbf{r},\mathbf{\Omega},t) \tag{5}$$

of the laser profile and the atomic profile (see, for instance, [5]), with

$$b(x,v_x)=d_2\frac{B_{12}}{4\pi^2}\left\{\left[\nu_L\left(1+\frac{v_x}{c}\right)-\frac{E_{12}(x)}{h}\right]^2+d_2^2\right\}^{-1}. \tag{6}$$

This coefficient $b(x,v_x)$ contains both the Stark effect and the Doppler effect and regulates the interaction between atoms and photons within the slab. It has the meaning of a cross section. At a position x, only particles with velocities $v_x\in[v_{\min}=v_{\rm res}(L),v_{\max}=v_{\rm res}(0)]$ interact with photons. The resonance speed is given by

$$v_{\rm res}(x)=c\left[\frac{E_{12}(x)}{h\nu_L}-1\right]. \tag{7}$$

By inserting Eq. (4) into Eq. (6) and setting $v_{\min}=0$, we obtain, after some algebra,

$$b(x,v_x)=v_2\frac{B_{12}c}{4\pi^2\nu_L}\left\{\left[v_x-v_{\max}\left(1-\frac{x}{L}\right)\right]^2+v_2^2\right\}^{-1}, \tag{8}$$

where v_2 is the natural linewidth expressed in velocity space.

B. Discretization

Photons are allowed to attain only four directions in the plane (x,y):

$$\mathbf{e}_1=-\mathbf{e}_3=\mathbf{i},\quad \mathbf{e}_2=-\mathbf{e}_4=\mathbf{j},$$

where $\mathbf{e}_i$ is a unit vector (laser photons have direction $\mathbf{e}_3$). Atoms A and A^* can attain only velocities that belong to the following lattice in the plane (x,y):

$$\mathbf{v}_{k,\ell}=(k\mathbf{i}+\ell\mathbf{j})\Delta v, \tag{9}$$

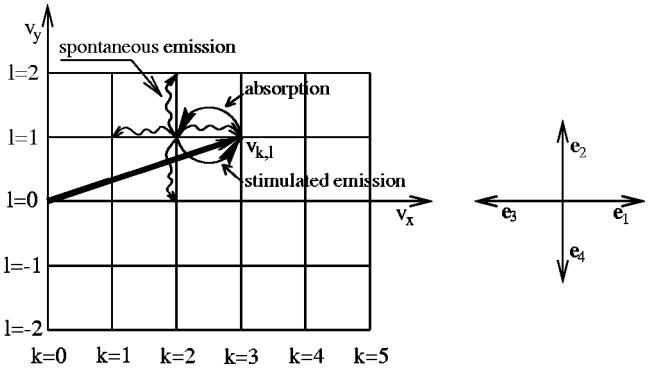

FIG. 1. Possible events for photon-atom interactions. On the left-hand side the velocity lattice for atoms A and A^* is shown. On the right-hand side the velocity vectors for photons are presented.

where $k \in \mathbb{Z}$, $\ell \in \mathbb{Z}$ ($\mathbb{Z}$ is the set of relative integers), and $\Delta v = h\nu_L/mc$, which is the change of the velocity of an atom due to atom-photon interaction (Fig. 1). We denote by (k,ℓ) and $(k,\ell)^*$ atoms A and A^*, respectively, which have a velocity $\mathbf{v}_{k,\ell}$. Here p_s is a photon with direction $\mathbf{e}_s$ ($s=1,2,3,4$).

We neglect the interactions of secondary photons with atoms. By taking into account momentum conservation, the following events are possible: *absorption*

$$(k,\ell)+p_3 \rightarrow (k-1,\ell)^*$$

and *stimulated emission*

$$(k,\ell)^*+p_3 \rightarrow (k+1,\ell)+2p_3.$$

According to momentum conservation, the following spontaneous emission events are allowed:

$$\begin{aligned}(k,\ell)^* &\rightarrow (k-1,\ell)+p_1' \\ &\rightarrow (k,\ell-1)+p_2' \\ &\rightarrow (k+1,\ell)+p_3' \\ &\rightarrow (k,\ell+1)+p_4'.\end{aligned}$$

According to the circularly polarized driving field, the output probability is 1/3 in the transversal direction and 2/3 in the longitudinal direction.

C. Equations of the model

The number densities of particles A and A^* at time t and position (x,y) with velocity $\mathbf{v}_{k,\ell}$ are $N_{k,\ell}(x,y,t)$and $N^*_{k,\ell}(x,y,t)$, respectively. The intensity $I_s(x,y,t)$ ($s=1,2,3,4$) is the number of photons p_s per unit volume multiplied by $ch\nu_L$ in the direction s. There is a zero Doppler effect for photons 2 and 4 and a negative Doppler effect for photon 1. Furthermore, we are only interested in stationary solutions of the problem. We can therefore write down the kinetic equations for particles A and A^*. For *particles* (k,ℓ),

$$\mathbf{v}_{k,\ell}\cdot\nabla N_{k,\ell} = \mathcal{J}^{a}_{k,\ell}+\mathcal{J}^{\mathrm{sp}}_{k,\ell}+\mathcal{J}^{\mathrm{st}}_{k,\ell}, \tag{10}$$

where the interaction contributions due to absorption (a), spontaneous (sp), and stimulated (st) emission are given by

$$\mathcal{J}^{a}_{k,\ell} = -b_k(x)I_3N_{k,\ell}, \tag{11a}$$

$$\mathcal{J}^{\mathrm{sp}}_{k,\ell} = \frac{A_{12}}{4}(N^*_{k+1,\ell}+N^*_{k-1,\ell}+N^*_{k,\ell+1}+N^*_{k,\ell-1}), \tag{11b}$$

$$\mathcal{J}^{\mathrm{st}}_{k,\ell} = b_{k-1}(x)I_3N^*_{k-1,\ell}, \tag{11c}$$

with $b_k(x)=b(k\Delta v,x)$. For *particles* $(k,\ell)^*$,

$$\mathbf{v}_{k,\ell}\cdot\nabla N^*_{k,\ell} = \mathcal{J}^{a,*}_{k,\ell}+\mathcal{J}^{\mathrm{sp},*}_{k,\ell}+\mathcal{J}^{\mathrm{st},*}_{k,\ell}, \tag{12}$$

where

$$\mathcal{J}^{a,*}_{k,\ell} = b_{k+1}(x)I_3N_{k+1,\ell}, \tag{13a}$$

$$\mathcal{J}^{\mathrm{sp},*}_{k,\ell} = -A_{12}N^*_{k,\ell}, \tag{13b}$$

$$\mathcal{J}^{\mathrm{st},*}_{k,\ell} = -b_k(x)I_3N^*_{k,\ell}. \tag{13c}$$

D. Consideration of $b_k(x)$

In general, $v_{\mathrm{res}}(x)$ does not belong to the grid because $v_{\mathrm{res}}(x)/\Delta v$ is not an integer. In order to ensure that the maximum of $b(x,v_x)$ with respect to v_x corresponds to a grid point at each position x, it is necessary to introduce a stepwise approximation $\tilde{v}_{\mathrm{res}}(x)$ of $v_{\mathrm{res}}(x)$ such that $\tilde{v}_{\mathrm{res}}(x)/\Delta v$ is always an integer:

$$\tilde{v}_{\mathrm{res}}(x) = \Delta v\left[\frac{v_{res}(x)}{\Delta v}\right]^*, \tag{14}$$

where $[z]^*$ is the integer part of z.

The stepwise approximation $\tilde{E}_{12}(x)$ of $E_{12}(x)$, given by

$$\begin{aligned}\tilde{E}_{12}(x) &= h\nu_L\left(1+\frac{\tilde{v}_{\mathrm{res}}(x)}{c}\right) \\ &= h\nu_L\left\{\frac{\Delta v}{c}\left[\frac{c}{\Delta v}\left(\frac{E_{12}(x)}{h\nu_L}-1\right)\right]^*+1\right\},\end{aligned} \tag{15}$$

corresponds to $\tilde{v}_{\mathrm{res}}(x)$. Finally, one can write

$$b_k(x) = \begin{cases} B\{\gamma[k-\tilde{k}(x)]\}, & \text{for } k_0 \leqslant k \leqslant k_L \\ 0 & \text{otherwise,}\end{cases} \tag{16}$$

where $\gamma = \nu_L\Delta v/c$, $\tilde{k}(x)=\tilde{v}_{\mathrm{res}}(x)/\Delta v$, $k_0=\tilde{k}(0)$, and $k_L=\tilde{k}(L)$. Consequently, we have

$$\mathcal{J}^{a}_{k,\ell} \neq 0 \quad \text{for } k_0 \leqslant k \leqslant k_L,$$

$$\mathcal{J}^{\mathrm{st}}_{k,\ell} \neq 0 \quad \text{for } k_0+1 \leqslant k \leqslant k_L+1,$$

$$\mathcal{J}^{a,*}_{k,\ell} \neq 0 \quad \text{for } k_0-1 \leqslant k \leqslant k_L-1,$$

$$\mathcal{J}^{\mathrm{st},*}_{k,\ell} \neq 0 \quad \text{for } k_0 \leqslant k \leqslant k_L.$$

III. ONE-DIMENSIONAL CASE

With the model in mind, we want to study the one-dimensional case. Atoms enter the deceleration path in direction x counterpropagating to the laser beam. We assume that spontaneous emission only occurs in direction x or $-x$ and that the intensity I_3 is constant within the slab. Under these restrictions we can formulate the balance equations for atoms in the ground state,

$$k\Delta v \frac{d}{dx} N_k(x,y) = \frac{A_{12}}{2}(N^*_{k+1}+N^*_{k-1}) + b_{k-1}(x) I_3 N^*_{k-1} - b_k(x) I_3 N_k , \tag{17}$$

and the excited state,

$$k\Delta v \frac{d}{dx} N^*_k(x,y) = b_{k+1}(x) I_3 N_{k+1} - A_{12} N^*_k - b_k(x) I_3 N^*_k . \tag{18}$$

The coefficient 1/2 in Eq. (17) appears because photons can be emitted spontaneously only in two different directions. In order to obtain a system of coupled differential equations with constant coefficients, we divide the deceleration path into $k_0 = v_{\max}/\Delta v$ layers. The thickness of one layer is given by $\Delta x = L/k_0$. Within each layer $x' \in [0,\Delta x]$, the coefficients $b_k(x')$ do not depend on the spatial variable x' due to the requirements on $b_k(x)$ in Sec. II D.

In each layer of the deceleration path, only atoms within the resonance range are able to interact with photons. The probability of an interaction is given by $b_k(x)$. All other atoms are not affected, i.e., the corresponding number densities do not change. This reduces the number of differential equations dramatically.

The reduced system corresponding to the jth layer can be written as

$$\frac{d}{dx} \hat{\mathbf{N}}^{(j)} = M^{(j)} \hat{\mathbf{N}}^{(j)}, \tag{19}$$

where $\hat{\mathbf{N}}^{(j)}$ is a vector including only the number densities of affected atoms in the ground state and in the excited state. The sparse coefficient matrix $M^{(j)}$ results from the coupled systems [Eqs. (17) and (18)] of differential equations, however, in its reduced form. The numbering of the components of the density vector is done in such a way that the entries of the matrix $M^{(j)}$ are very close to the main diagonal. Calculating the eigenvalues $z_n^{(j)}$ and the eigenvectors $\mathbf{V}_n^{(j)}$ of the matrix $M^{(j)}$, we obtain the solution vector

$$\hat{\mathbf{N}}^{(j)}(x') = \sum_{n=1}^{S} c_n^{(j)} \mathbf{V}_n^{(j)} \exp(z_n^{(j)} x'), \tag{20}$$

where S is the size of the matrix depending on the chosen discretization. The density distributions of each layer are connected by means of the condition of continuity

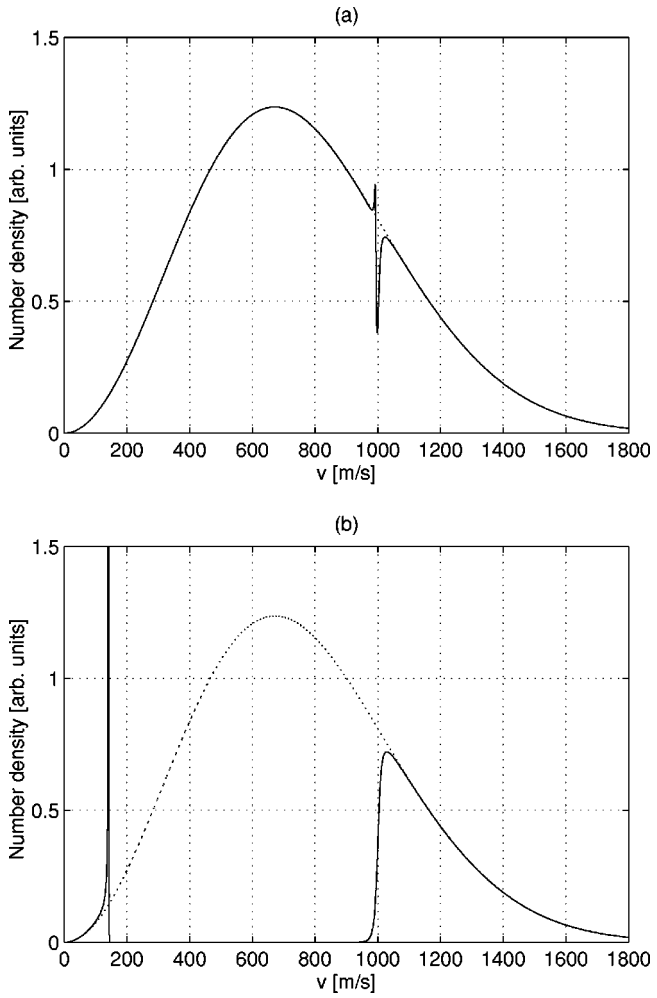

FIG. 2. (a) Velocity distribution of atoms in the ground state for the saturation case ($I_3 = I_{\text{sat}}$) at $x = 3.2$ mm. (b) Depletion of the distribution at $x = 552.5$ mm. The dotted curve is the original Maxwell distribution at $x = 0$.

$$\mathbf{N}^{(j)}(x' = \Delta x) = \mathbf{N}^{(j+1)}(x' = 0), \tag{21}$$

where $\mathbf{N}^{(j)}$ $(j = 1, \ldots, k_0)$ represents the nonreduced density vectors. The coefficients $c_n^{(j)}$ in Eq. (20) result from

$$\mathbf{C}^{(j)} = [V^{(j)}]^{-1} \hat{\mathbf{N}}^{(j)}(x' = 0), \tag{22}$$

where $[\mathbf{C}^{(j)}]^t = (c_1^{(j)}, \ldots, c_S^{(j)})$ and $[V^{(j)}]^{-1}$ is the inverse matrix of $V^{(j)} = (\mathbf{V}_1^{(j)}, \ldots, \mathbf{V}_S^{(j)})$. For the first layer $\mathbf{N}^{(1)}(x' = 0)$ is a given velocity distribution.

IV. SEMIANALYTICAL RESULTS

In this section the one-dimensional procedure of the above-mentioned layer method is applied to a special case. Let us consider sodium atoms in the ground state $3\,^2S_{1/2}$ and the excited state $3\,^2P_{3/2}$. The corresponding transition is the D_2 line. Maxwellian distributed sodium atoms at the ground state emerge from an oven at a temperature of $T = 625$ K. Collimated to an atomic beam, they enter the interaction zone at $x = 0$. The typical length of the deceleration path in experiments is given by $L = 650$ mm. Absorption or emission of a photon changes the value of the speed of a sodium

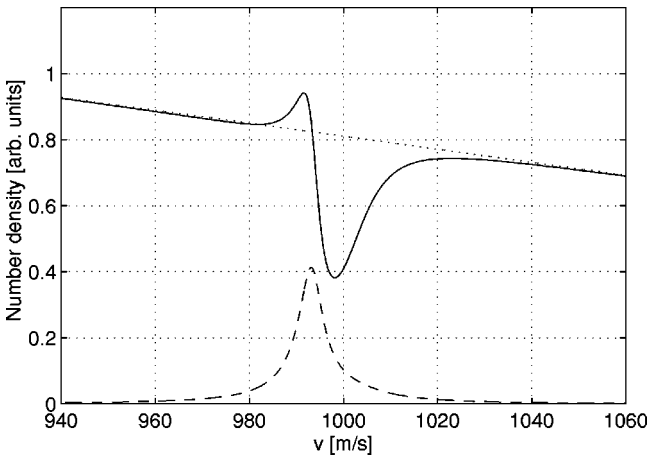

FIG. 3. Resolved velocity distribution of ground level atoms (solid curve) and excited atoms (dashed-dotted curve) at $x=3.2$ mm. The dotted curve is the original Maxwell distribution at $x=0$.

atom by an amount $\Delta v=2.94$ cm/s. Starting at an initial velocity of $v_0=1000$ m/s, one needs approximately 35 000 discretization points to cover the interesting velocity range.

Due to the slow decay of the wings of the atomic Lorentzian profile, one needs a relatively wide velocity range to take into account all essential atom-photon interactions. Therefore, we obtain a system of approximately 40 000 differential equations. The solution described in the above section is important for theoretical considerations. Numerically, it is more straightforward to apply an exponential matrix formalism for solving the system of differential equations. Hence we use a series representation to replace the exponential matrix and end the calculation if the norm of the remainder is below a required relative error.

A. Saturation and cooling limit

First, we consider the saturation case, where the intensity of the laser beam I_3 is sufficiently high ($I_3=I_{\mathrm{sat}}$) such that all ground level atoms within the interaction range are

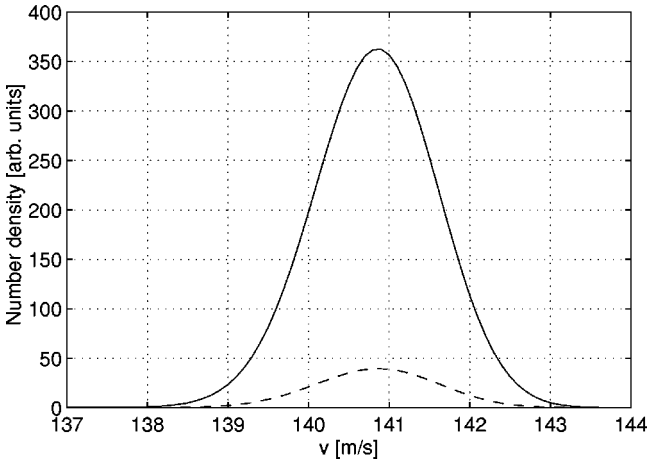

FIG. 4. Resolved cooling peak of ground level atoms (solid curve) at $x=552.5$ mm. The width of the peak is given by $\delta v=2.26$ m/s. The dashed-dotted curve represents the velocity distribution of the excited atoms.

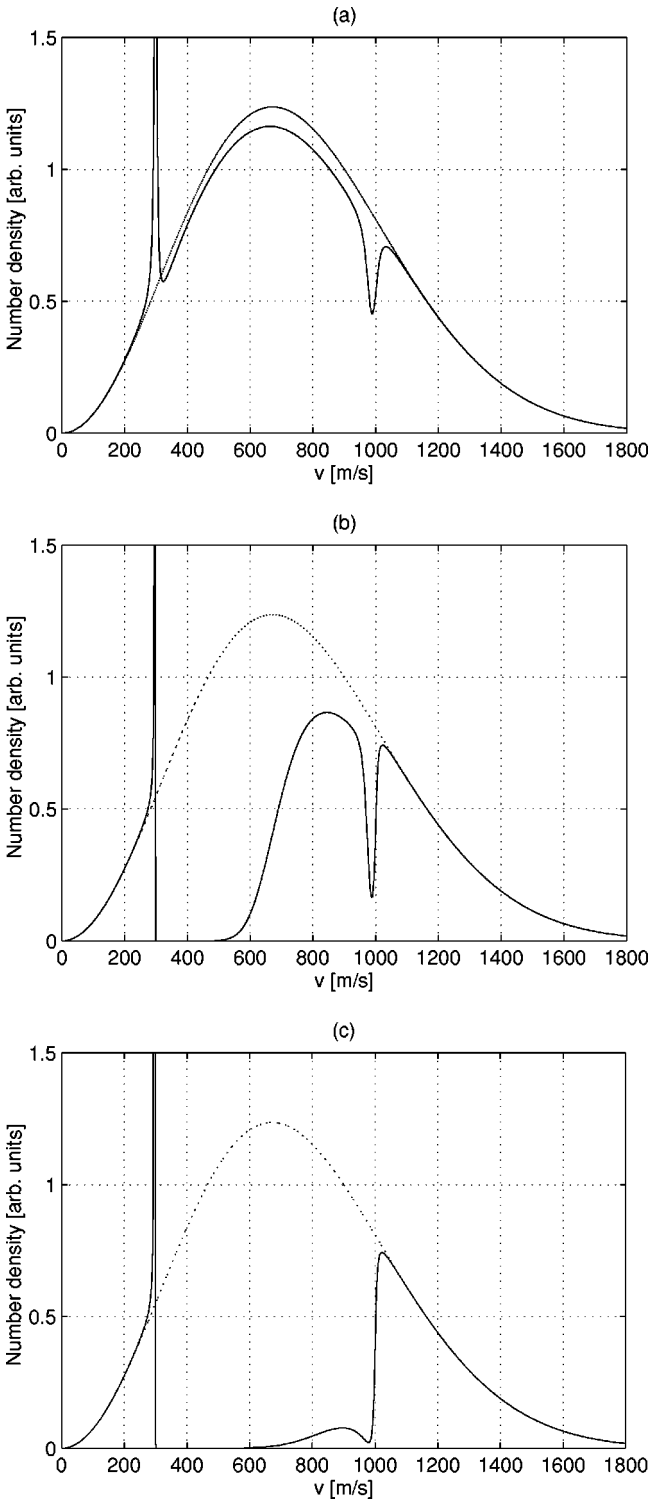

FIG. 5. Velocity distributions of ground level atoms (solid curve) at $x=455$ mm for different intensities of the laser beam. The dotted curve represents the original Maxwell distribution. (a) $I_3=\frac{1}{4}I_{\mathrm{sat}}$, (b) $I_3=\frac{1}{2}I_{\mathrm{sat}}$, and (c) $I_3=\frac{3}{4}I_{\mathrm{sat}}$.

slowed. Figures 2(a) and 2(b) show the change of the Maxwell distribution of the ground level atoms during the cooling process. Fast atoms are slowed to lower velocities generating the so-called cooling peak [Fig. 2(a)]. The successively growing cooling peak moves with increasing x from $v=v_0$ to $v=v_{\min}$ [Fig. 2(b)]. A resolution of the cooling peak of the ground level atoms (solid curve) as well as of

the excited atoms (dash-dotted curve) at $x=3.2$ mm is displayed in Fig. 3. The peak of the excited atoms is asymmetrical because atoms out of the resonance range decay only spontaneously. The cooling peak at the end of the interaction zone (Fig. 4) is a Gaussian-like, bell-shaped curve. The width of the peak is a measure of the efficiency of laser cooling. The average kinetic energy of the particles within the cooling peak and therefore also the kinetic temperature

$$T=\frac{m}{k_B f}\frac{\sum_{i=0}^{\infty} N_i(v_i-u)^2}{\sum_{i=0}^{\infty} N_i} \tag{23}$$

is very low. Here m is the mass of the atoms, k_B is Boltzmann's constant, u denotes the mean velocity, and f is the number of degrees of freedom. For the chosen discretization, we obtain a temperature of $T=3520\ \mu$K, which is in good agreement with $T=4300\ \mu$K [13] obtained by quantum mechanical calculations.

The lowest possible temperature, the so-called cooling limit, depends mainly on the form of the atomic profile. Supposing a step function instead of the Lorentzian profile, the width of the so-obtained cooling peak is exactly Δv (recoil limit).

B. Low intensities

In the case of low intensities, not all atoms within the resonance range interact with photons. Many atoms remain in their velocity classes. When the intensity approaches zero, the Maxwell distribution is not changed. Figures 5(a)–5(c) show how increasing intensities change the Maxwell distribution during the cooling process. If the intensity is very low $I_3=\frac{1}{4}I_{\mathrm{sat}}$, as in Fig. 5(a), the resulting velocity distribution is characterized by a notch at v_0, a cooling peak at low velocities, and a nearly unchanged distribution in between. The typical notch at v_0 arises because at first, fast atoms are slowed and form a peak at a little bit lower velocities. Then this peak increases and simply moves to lower velocities. For higher intensities $I_3=\frac{1}{2}I_{\mathrm{sat}}$ [Fig. 5(b)], the cooling peak and the peak of the excited atoms increase. Because of a greater interaction probability per unit path length for atoms with lower velocities, increasingly more atoms are slowed. At an intensity of $I_3=\frac{3}{4}I_{\mathrm{sat}}$ [Fig. 5(c)] almost all atoms are affected by the cooling process. Only a few fast atoms have a chance to escape an interaction with photons.

V. CONCLUSION

This paper treats the mechanism of atom-photon interaction from a statistical point of view. In particular, the mechanism studied here allows one to describe radiation pressure effects of resonant light on free atoms. For the scenario of a Stark effect laser cooling device, a discrete velocity model of the Boltzmann equation is developed. It leads to a system of coupled differential equations governing the number densities of atoms for each discrete velocity. A velocity- and space-dependent cross section, resulting from the Stark and the Doppler effect by taking into account the atomic and laser profile, regulates the slowing of atoms. By dividing the interaction zone into a high number of very thin layers, the coefficients of the differential equations become constant and its solution can be represented as a superposition of exponential functions. The obtained velocity distribution of slowed atoms at each point of the deceleration path is studied in detail. Also the influence of the laser intensity on the net momentum transfer from the laser photons to the atoms is investigated.

We would like to emphasize that our semianalytic method is precise and much more efficient than a solution by means of a Runge-Kutta algorithm. It turns out that in the case of a Runge-Kutta integration it is impossible to overcome the stepsize and storage problems resulting from the occurrence of very sharp peaks of the solution functions.

We plan to extend our numerical computations to higher-dimensional configuration spaces and velocity spaces in order to treat transversal heating. Furthermore, it should be possible to deal with multilevel systems and to take into account the variation of the photon field.

ACKNOWLEDGMENTS

This work was partially supported by the Consiglio Nazionale delle Ricerche (CNR-GNFM) and by the Fonds zur Förderung der wissenschaftlichen Forschung, Vienna, under Contract No. P10879-TEC.

[1] C. Cercignani, *The Boltzmann Equation and Its Applications*, Vol. 67 of *Applied Mathematical Sciences* (Springer-Verlag, New York, 1988).
[2] C. R. Garibotti and G. Spiga, J. Phys. A **27**, 2709 (1994).
[3] J. W. Bond, K. M. Watson, and J. A. Welch, *Atomic Theory of Gas Dynamics* (Addison-Wesley, Reading, MA, 1965).
[4] S. I. Pai, *Radiation Gas Dynamics* (Springer-Verlag, Wien, 1969).
[5] J. Oxenius, in *Kinetic Theory of Particles and Photons,* edited by G. Ecker, W. Engl, and L. B. Felsen, Springer Series on Electrophysics Vol. 20 (Springer-Verlag, Berlin, 1986).
[6] A. Rossani, G. Spiga, and R. Monaco, Mech. Res. Commun. **24**, 237 (1997).
[7] H. Cabannes (unpublished).
[8] R. Monaco and L. Preziosi, *Fluid Dynamic Applications of the Discrete Boltzmann Equation* (World Scientific, Singapore, 1991).
[9] J. A. Broadwell, Phys. Fluids **7**, 1243 (1964).
[10] R. Gatignol, in *Théorie Cinétique oles Gaz a Répartition Discrète de Vitesses*, Lecture Notes in Physics, Vol. 36 (Springer-Verlag, Berlin, 1975).
[11] H. Cabannes, J. Mec. **14**, 705 (1975).

[12] H. Cornille, Transp. Theory Stat. Phys. **26**, 359 (1997).
[13] R. Blatt, W. Ertmer, P. Zoller, and J. L. Hall, Phys. Rev. A **34**, 3022 (1986).
[14] W. D. Phillips, in *Laser Manipulation of Atoms and Ions*, Proceedings of the International School of Physics ''Enrico Fermi,'' Course CXVIII, Varenna, Amsterdam, 1991, edited by E. Arimondo, W. D. Phillips, and F. Strumia (North-Holland, Amsterdam, 1992).
[15] R. J. Cook and A. Ashkin, Phys. Rev. A **21**, 1606 (1980).
[16] V. G. Minogin, Zh. Éksp. Teor. Fiz. **79**, 2044 (1980) [Sov. Phys. JETP **52**, 1032 (1980)].
[17] S. Stenholm, Phys. Rev. A **27**, 2513 (1983).
[18] H. Risken, *The Fokker-Planck Equation* (Springer-Verlag, Berlin, 1983).
[19] H. Wallis and W. Ertmer, J. Phys. B **21**, 2999 (1988).